

# DETERMINISTIC METHODS FOR TIME-DEPENDENT STOCHASTIC NEUTRON TRANSPORT

**Randal S. Baker**

Los Alamos National Laboratory  
MS D409, Los Alamos, NM 87545  
rsb@lanl.gov

## ABSTRACT

A numerical method is presented for solving the time-dependent survival probability equation in general (1D/2D/3D) geometries using the multigroup  $S_N$  method. Although this equation was first formulated by Bell in the early 1960's, it has only been applied to stationary systems (for other than idealized point models) until recently, and detailed descriptions of numerical solution techniques are lacking in the literature. This paper presents such a description and applies it to a dynamic system representative of a figurative criticality accident scenario.

*Key Words:* Stochastic Neutron Transport, Probability of Initiation, Survival Probability

## 1. INTRODUCTION

In his classic 1965 paper, Bell [1] derived the generating function for determining the probability distribution of obtaining exactly  $n$  neutrons at some point in space, time, angle, and energy. Bell showed that while the mean of this equation leads to the standard Boltzmann transport equation, higher-order moments can be used to determine the variance of the neutron population, or the probability of getting a divergent chain reaction from an initial neutron, i.e., survival probability. As the survival probability equation may be viewed as essentially an adjoint, time-dependent transport equation, but with additional coupled non-linear terms, solutions are even more difficult to come by than for the standard transport equation, and so until recently numerical solutions have been limited to stationary systems [2,3] for other than idealized point models [4]. For a stationary system, the probability of a neutron surviving until an infinite time is only greater than zero for a super-critical system, and hence these solutions came to be referred to as "Probability of Initiation". In reality, however, criticality accidents involve dynamically changing configurations and, as will be shown here, there can be significant differences between interpretations of the stationary and dynamic solutions that might affect accident analysis.

Despite Bell's suggestion in [1] that numerical techniques such as the  $S_N$  method then under development by Carlson [5] would be well-suited for this problem, to this author's knowledge Humbert [6] was the first to apply deterministic transport methods to the solution of the time-dependent survival probability equation. However, his paper contained no details on the numerical solution techniques employed to ensure convergence, and results were presented for a stationary system only. Here, we will describe the techniques we have found necessary for fast and reliable convergence on a variety of applications and initial conditions, and examine how well they perform on a figurative dynamic criticality accident scenario. We will also examine the

differences between the stationary and dynamic solutions for this scenario and discuss their implications.

## 2. SOLUTION TECHNIQUES FOR THE TIME-DEPENDENT SURVIVAL PROBABILITY EQUATION

The survival probability equation derived by Bell [1] for the probability  $p$  that some neutron at a point  $\bar{r}$  in space, in direction  $\bar{\Omega}$ , with energy  $E$ , and at time  $t$ , or its progeny, will survive to some final time  $t_F$  is essentially a time-dependent adjoint equation with additional non-linear terms that depend upon the probability  $P_j$  of  $j$  neutrons being emitted from any given fission. Incorporating this probability  $P_j$  into the term  $\Lambda_j$ , and neglecting delayed and  $(n, xn)$  neutrons, this equation is

$$\begin{aligned}
 & -\frac{1}{v} \frac{\partial}{\partial t} p(\bar{r}, \bar{\Omega}, E, t) - \bar{\Omega} \cdot \nabla_{\bar{r}} p(\bar{r}, \bar{\Omega}, E, t) + \Sigma_T(\bar{r}, E, t) p(\bar{r}, \bar{\Omega}, E, t) = \\
 & \int_0^\infty \int_{4\pi} dE' d\bar{\Omega}' \Sigma_s(\bar{r}, \bar{\Omega}, E, t \rightarrow \bar{\Omega}', E') p(\bar{r}, \bar{\Omega}', E', t) + \\
 & v \Sigma_F(\bar{r}, E, t) \int_0^\infty \int_{4\pi} dE' \frac{d\bar{\Omega}'}{4\pi} \chi(\bar{r}, E \rightarrow E') p(\bar{r}, \bar{\Omega}', E', t) - \\
 & \sum_j (-1)^j \Lambda_j(\bar{r}, E, t) \left( \int_0^\infty \int_{4\pi} dE' \frac{d\bar{\Omega}'}{4\pi} \chi(\bar{r}, E \rightarrow E') p(\bar{r}, \bar{\Omega}', E', t) \right)^j, \quad (1) \\
 & p(\bar{r}_B, \bar{\Omega}, E, t) = 0, \quad \bar{\Omega} \cdot \hat{n} > 0.
 \end{aligned}$$

Putting this equation into multigroup form (group  $g$ ) with Crank-Nicholson in time ( $p(t_n^*) \equiv p_n$ ), and suppressing the space and angle dependence, we obtain

$$\underline{L}_g^* p_{gn} + \frac{2}{v_g \Delta t_n} p_{gn} = \sum_{g'} \underline{S}_{g' \rightarrow g}^* p_{g'n} + Q_{gn} + \frac{2}{v_g \Delta t_n} p_{gn-1/2}, \quad t^* : t_F \rightarrow 0 \quad (2a)$$

$$Q_{gn} = v \Sigma_{F,g} F_{gn}[p_n] - \sum_{j=2}^J (-1)^j \Lambda_{jg} (F_{gn}[p_n])^j \quad (2b)$$

$$F_{gn}[p_n] = \sum_{g'=1}^G \int_{4\pi} \frac{d\bar{\Omega}'}{4\pi} \chi_{g \rightarrow g'} p_{g'n} \quad (2c)$$

$$\Lambda_{jg} = v \Sigma_{F,g} \frac{\sum_{l=j}^\infty \text{perm}(l, j) P_{lg}}{j! \sum_j j P_{jg}} \quad (2d)$$

Here, standard adjoint reversals in direction and energy have been applied to the streaming/removal and scattering operators  $\underline{L}$  and  $\underline{S}$ , respectively. Solution of an adjoint time-dependent equation also requires a reversal in time, which we perform by defining the adjoint time  $t^* \equiv t_F - t$  and requiring an ‘‘initial’’ condition  $p(t_F)$ . The  $J$  in Eq. (2b) is the maximum

number of fission neutrons emitted in fission (typically 5-10). Material properties (including those of the fission multiplicity terms in  $Q$ ) are assumed to be constant within a time step  $\Delta t_n$ , and  $\int_{\Delta t_n} F_g^j(t) dt \approx F_{gn}^j \Delta t_n$ . Thus, while the temporal (and spatial) discretizations used are second-order in nature, the assumption of constant material properties within a time step introduces a first-order error term, the importance of which will be problem-dependent.

As posed above, the survival probability equation is a non-linear inhomogeneous source equation which we solve by replacing the standard outer iteration on fission with a “lambda” iteration  $k$  on a fictitious “inhomogeneous source” term  $Q$

$$\underline{L}_g^* p_{gn}^k + \frac{2}{v_g \Delta t_n} p_{gn}^k = \sum_{g'} S_{g' \rightarrow g}^* p_{g'n}^k + Q_{gn}^{k-1} + \frac{2}{v_g \Delta t_n} p_{gn-1/2} \quad (3a)$$

$$Q_{gn}^{k-1} = v \Sigma_{F,g} F_{gn} [p_n^{k-1}] - \sum_{j=2}^J (-1)^j \Lambda_{jg} (F_{gn} [p_n^{k-1}])^j, \quad Q_{gn}^0 = Q_{gn-1}^K. \quad (3b)$$

Similar to the approach used in [7] for stationary systems, we apply a global re-balance after every lambda iteration to ensure/accelerate convergence. The re-balance is done by letting  $p_{gn} \rightarrow \lambda p_{gn}^k$  in Eq. (2), then subtracting off Eq. (3), resulting in

$$\sum_g Q_{gn}^{k-1} - \sum_g v \Sigma_{F,g} F_{gn} [p_n^k] + \frac{\lambda-1}{\lambda} \sum_g \frac{2}{v_g \Delta t_n} p_{gn-1/2} + \sum_{j=2}^J (-1)^j \lambda^{j-1} \sum_g \Lambda_{jg} (F_{gn} [p_n^k])^j = 0 \quad (4)$$

This order  $J$  non-linear equation for  $\lambda$  is solved using a modified Powell hybrid method [8]. The resulting  $\lambda p_{gn}^k$  are then used to form  $Q_{gn}^{k-1}$  for the next lambda iteration. Lambda iterations are continued until  $|1 - \lambda| < \varepsilon$  and  $|1 - F^k / F^{k-1}| < \varepsilon$ . Following convergence, one additional lambda iteration is performed with no scaling to calculate consistent  $p_{n+1/2}$  and  $Q_{gn}^K$  for the next cycle. Inner iterations over the scattering source are accelerated using Diffusion Synthetic Acceleration.

### 3. “INITIAL” (FINAL) CONDITIONS

For systems where the final configuration is both static and supercritical  $p_{1/2}$  may be determined by setting it to the solution of the stationary “Probability of Initiation” problem  $p_0$ . We refer to this as a “settle” initial condition. Otherwise, recognizing that the survival probability  $p$  is defined as the probability of a neutron surviving until some  $t_F$ , and all neutrons present at  $t_F$  have (by definition) survived until  $t_F$ , then our “given” initial condition must be  $p(t_F) = p_{1/2} = 1$ . While the value of  $p(t_F)$  is thus uniquely determined, the selection of  $t_F$  is itself arbitrary. The impact of this will be shown in the following test problems.

### 4. RESULTS

In [3], results were presented for a suite of historical test problems (stationary bare spheres of plutonium or highly enriched uranium of varying density and radii) for various codes from LLNL and LANL, including LLNL’s continuous energy Monte Carlo transport code Mercury

[9] and LANL's  $S_N$  transport code PARTISN [10]. The uranium test problems' static single particle initiation probabilities defined by

$$P_S = \iiint S(\vec{r}, E, \vec{\Omega}) p(\vec{r}, E, \vec{\Omega}) d\vec{r} dE d\vec{\Omega}, \quad (5)$$

where  $\iiint S(\vec{r}, E, \vec{\Omega}) d\vec{r} dE d\vec{\Omega} = 1$ , are shown below in Table I. The PARTISN calculations were run using LANL's NDI library [11] and its fission multiplicity data with 30 energy groups,  $S_{16}$ ,  $P_4$  Legendre expansion, a Watt fission spectrum for  $S$ , and  $J=8$ .

**Table I.  $P_S$  for Highly Enriched Uranium Bare Spheres**

$\rho^*r$	Mercury $P_S$	PARTISN $P_S$
165	0.0000	0.0000
195	0.0914	0.0935
225	0.1710	0.1720
255	0.2328	0.2362
285	0.2877	0.2894
315	0.3319	0.3339

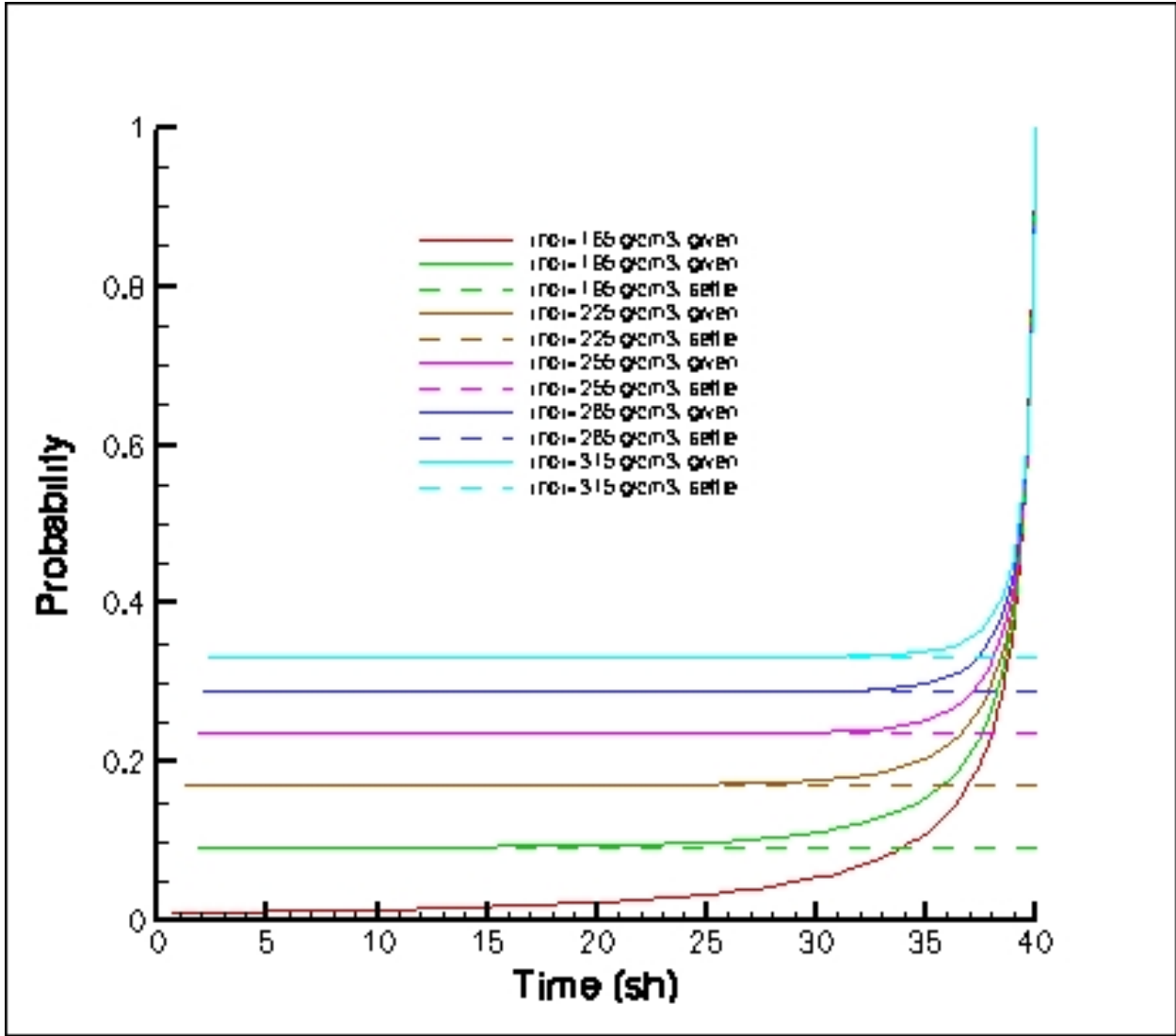
Note that the configuration with a density\*radius of 165 is sub-critical, thus the probability of a particle surviving for an infinite time is zero, and there is excellent agreement between Mercury and PARTISN for all test problems.

Figure 1 below shows the corresponding dynamic single particle initiation probabilities for these static problems. We define the dynamic single particle initiation probability as

$$P_S(t) = \iiint S(\vec{r}, E, \vec{\Omega}) p(\vec{r}, E, \vec{\Omega}, t) d\vec{r} dE d\vec{\Omega}. \quad (6)$$

We choose an “initial” (final) condition at forty shakes (1 sh =  $10^{-8}$  secs) using both the “settle” and “given” initial conditions discussed in Section 3 above. Since the “settle” initial (final) condition assumes a static geometry, the initial (final) dynamic probabilities reproduce the static probabilities and remain fixed at those values throughout the calculation. Thus, the “settle” initial condition may not be used for the  $\rho^*r = 165$  test case since it is sub-critical, and no static calculation is possible. In contrast, the “given” initial (final) condition at forty shakes sets  $p(\vec{r}, E, \vec{\Omega}, t_F)$ , and thus  $P_S(t_F)$ , equal to one. However, as the calculation proceeds (in the

reverse sense) towards  $t=0$ , and the transients introduced by this non-equilibrium initial condition die out, the dynamic probabilities come into agreement with their static probabilities.



**Figure 1. Dynamic Single Particle Initiation Probabilities, Bare HEU Spheres**

The outer “lambda” iteration scheme presented in Section 2 above required only 6-7 lambda iterations for the static test cases in Table I with a convergence criteria of  $10^{-4}$ . Historically, many static probability codes have encountered difficulties in convergence, i.e., excessive outer iterations, when attempting to determine static initiation probabilities for marginally critical systems. To examine how the global re-balance scheme used in PARTISN does for these systems we consider a modified version of our bare uranium sphere where the density is  $19.0 \text{ gm/cm}^3$ , the outer radius is  $8.7402094 \text{ cm}$ , and the calculated  $k_{eff}$  is 1.0001. For this marginally-critical configuration PARTISN requires, with a convergence criteria of  $10^{-4}$ , only eight lambda

iterations to calculate a  $P_S$  of  $7.1794 \times 10^{-5}$ . When the convergence criteria is tightened to  $10^{-8}$  only sixteen lambda iterations are required and  $P_S$  is identical to at least the first five digits. Based on this calculation, as well as other calculations not reported here, we conclude that the global re-balance scheme used in PARTISN does not appear to suffer from convergence difficulties for marginally-critical calculations.

Next, as a figurative criticality accident scenario, we consider a bare, 17.25 cm sphere composed of a 15 gm/cm<sup>3</sup> mixture of  $U^{235}$  and  $U^{238}$  where the isotopic weight fractions vary in time as  $U^{235}(14 - 6C_{MOD}) + U^{238}(1 + 6C_{MOD})$ . Figure 2 below shows the variation of  $C_{MOD}$  (and the corresponding  $k_{eff}$ ) as a function of time.

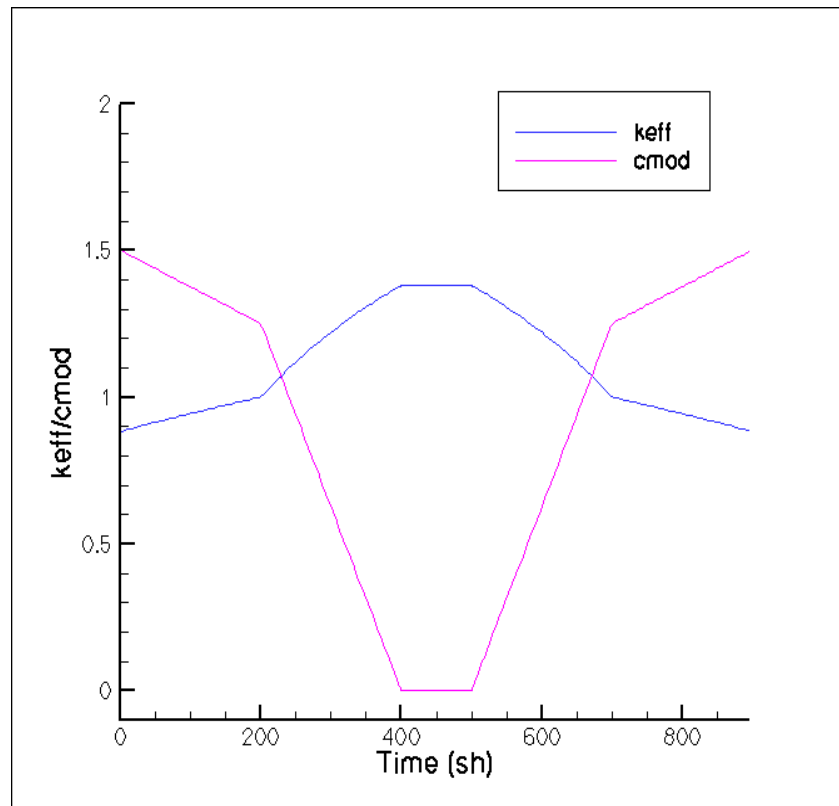


**Figure 2. Concentration/Criticality Variation**

Using 21 energy groups,  $S_{20}P_3$ ,  $J=6$ , a convergence criteria of  $10^{-6}$ , and a uniform source of 0.01 n/sh, we obtain the results shown in Fig. 3 below for a series of static “POI” calculations, a dynamic survival probability calculation using a “settle” initial condition near second criticality, and dynamic calculations with “given” initial conditions at  $t_F = 800, 100,$  and  $2000$  sh. Note that the static “POI” curve has the same symmetry as the concentration variation, but the dynamic calculations have varying degrees of asymmetry and, unlike the static calculation, indicate a non-zero probability for a neutron (or its progeny) “born” before first criticality surviving until after

second criticality. I.e., neutrons present in the system before first criticality can initiate chains that will persist (and multiply) throughout the criticality excursion until after second criticality. We see from Fig. 3 this can occur as early as 1  $\mu$ sec before initial criticality for this problem, and the probability is independent of the selected “initial” condition. Since these chains will undergo more multiplication than chains initiated shortly before second criticality, they are obviously of more significance for damage assessments.

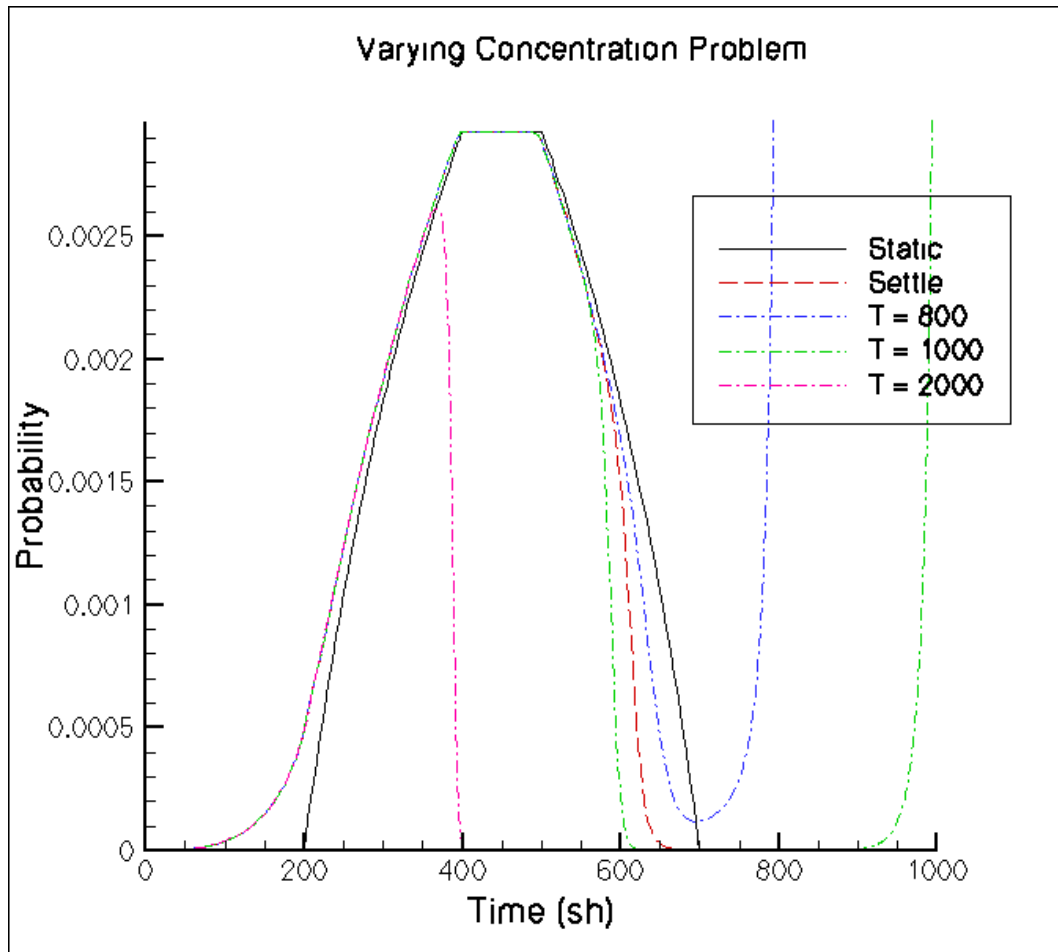


**Figure 3. Static/Dynamic Survival Probability for Varying Concentration**

At times immediately before second criticality all dynamic curves show a reduced probability of survival as compared to the static curve. This also agrees with physical intuition as neutron chains which initiate shortly before final criticality will undergo a smaller multiplication as compared to those initiated earlier, thus generating less neutrons which may survive until the specified final time. All “given” initial conditions show a non-physical, but mathematically meaningful, peak near their specified final time. This peak simply results from the definition of survival probability. That is, if our “initial” condition is  $p(t_F)=1$  at some specified final time, then the probability of a neutron surviving until that final time is also one. While the selection of this

final time is in some sense arbitrary, in reality it can be related to acceptable power generation levels during the excursion. That is, the probability for a neutron surviving a significant amount of time past second critical is larger if more neutrons are created during the criticality excursion.

The cumulative dynamic survival probability may be defined as

$$P_c(t) = 1 - \exp\left[-\iiint S(\vec{r}, E, \vec{\Omega}, t) p(\vec{r}, E, \vec{\Omega}, t) d\vec{r} dE d\vec{\Omega}\right] \quad (7)$$

and is shown below in Fig. 4 for this problem. The dynamic calculations, regardless of initial condition type or time, show a small but significant increase in the likelihood of a fission chain initiating at early times as compared to static POI calculations.

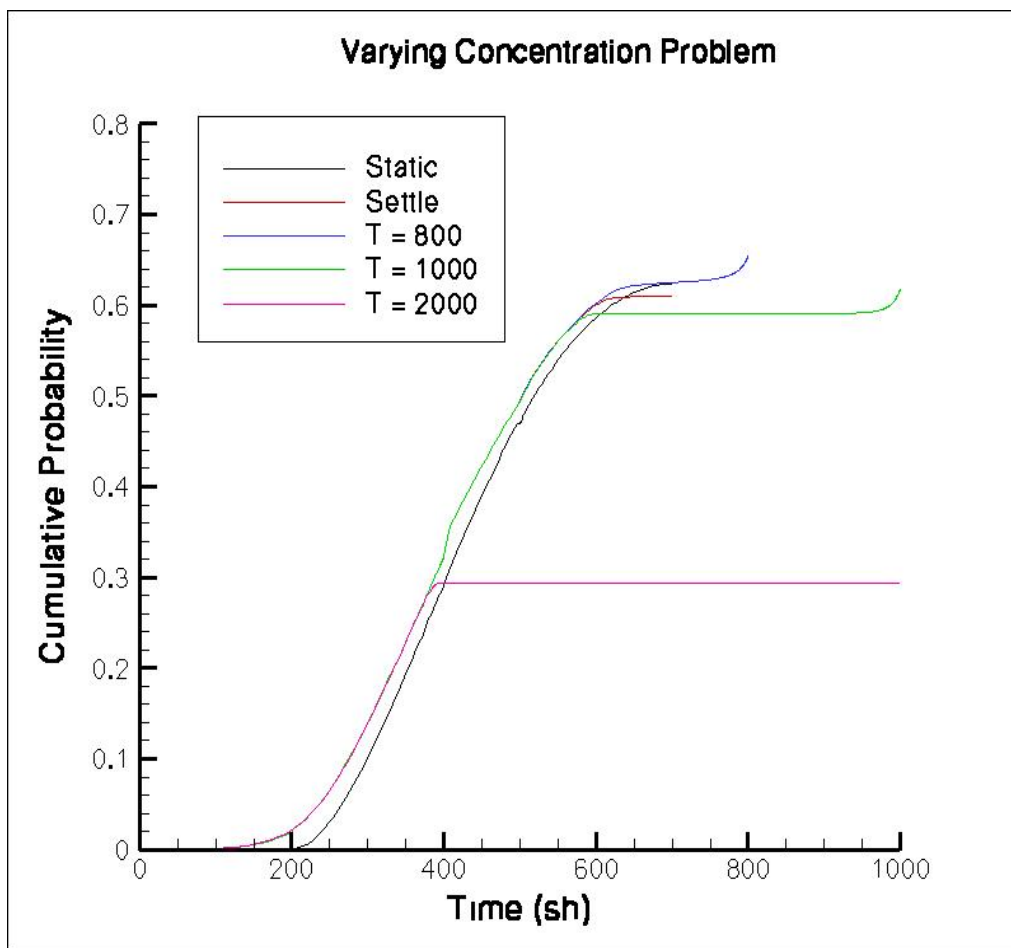


**Figure 4. Cumulative Survival Probability for Varying Concentration**

Finally, in Fig. 5 below, we show how the time step size and number of lambda iterations varies as a function of problem time for the case of the given initial condition at 800 sh. For survival probability calculations we use the maximum change in the point-wise total reaction rate to

govern whether the time step size is held constant, increased, or decreased. In addition, we force the time step to align with user-input parameter changes, in this case the concentration modifier changes at 200, 400, 500, and 700 sh. This has the effect of “crashing” the time step, as can clearly be seen below, from which it then recovers. In general, the number of lambda iterations per time step grows as the time step size increases, and also as the problem becomes more sub-critical, but decreases as criticality increases. However, even as  $k_{eff}$  varies between 0.88 and 1.38 for this problem, and with time steps ranging from 0.002 to 16.6 sh, we never require more than fourteen lambda iterations for convergence within a time step.

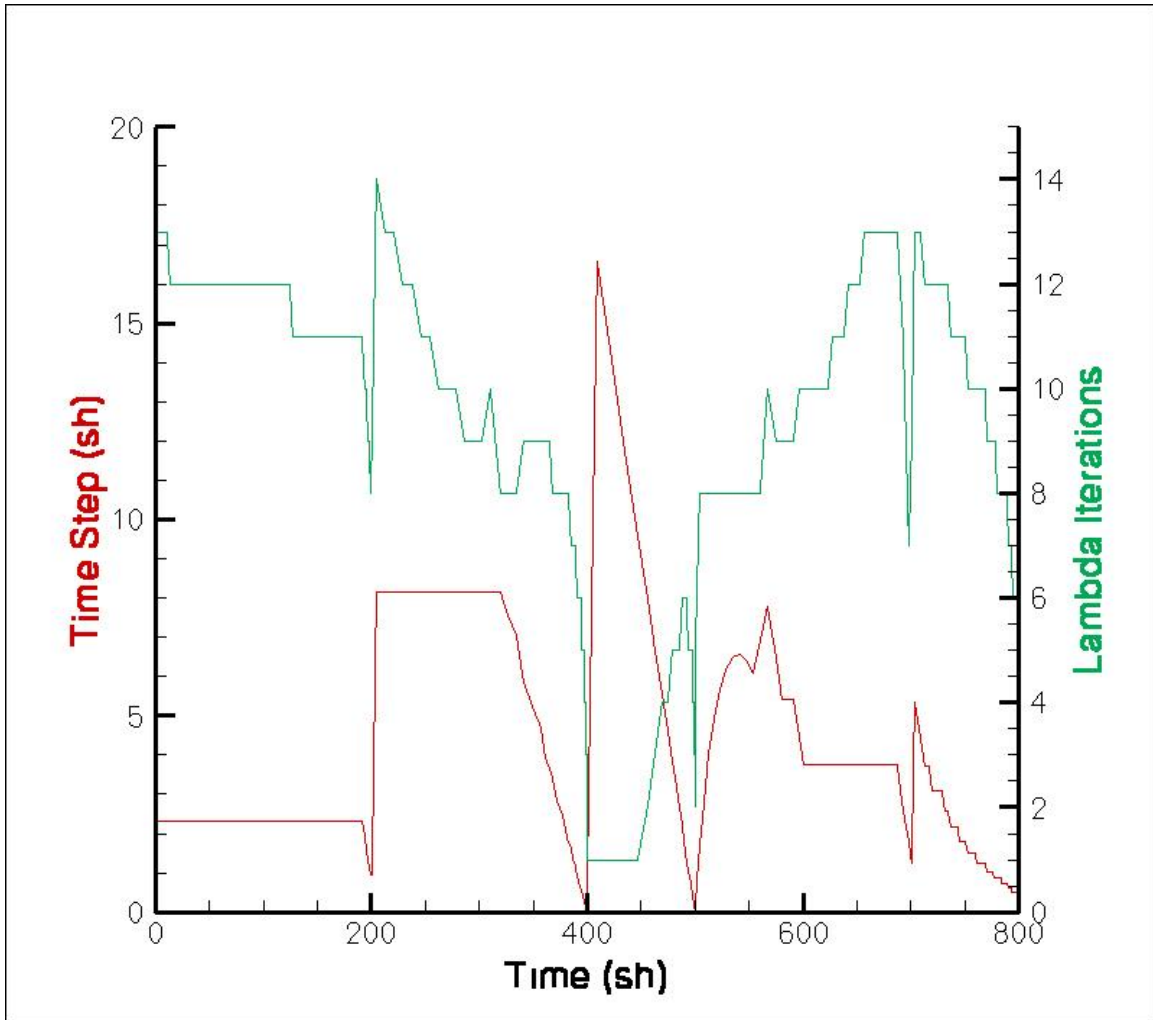


Figure 5. Time Step Size and Number of Lambda Iterations,  $t_F = 800$  sh

## 5. CONCLUSIONS

We have presented a detailed description of the numerical techniques we have found necessary for robust, accurate solutions of the dynamic survival probability equations using multigroup  $S_N$ .

Our results show that these solutions have the possibility to allow a more thorough understanding of criticality accident scenarios. We also note that by implementing these techniques in the LANL code PARTISN, a direct descendant of Carlson's original work at Los Alamos, we have, in some sense, finally completed Bell's conjecture about the applicability of Carlson's  $S_N$  methods to this problem [1].

We are currently adding the ability to obtain isotope-dependent spontaneous fission spectra and source strengths directly from LANL's NDI data library, rather than requiring users to enter it by hand. This will simplify the process of modeling more complex geometries. In the future, we hope to also incorporate the modifications required to the survival probability equations for neutrons generated by  $(n, xn)$  reactions. Finally, in order to model sub-prompt critical excursions, we will need to incorporate delayed neutrons as well.

### ACKNOWLEDGMENT

Los Alamos National Laboratory is operated by Los Alamos National Security, LLC for the United States Department of Energy under Contract No. DE-AC52-06NA25396.

### REFERENCES

1. George I. Bell, "On the Stochastic Theory of Neutron Transport," *Nucl. Sci. and Eng.*, **21**, pp.390-401 (1965).
2. Margaret W. Asprey and Clarence E. Lee, "DSN: A CDC-7600 FORTRAN Program for the Calculation of One-Dimensional, Multigroup Neutron Transport, Worth, and Persistent Fission Chain Probability," Los Alamos National Laboratory report LA-4897-DEL (1976).
3. G. M. Greenman, R. J. Procassini, and C. J. Clouse, "A Monte Carlo Method for Calculating Initiation Probability," *Joint Intl. Topical Mtg. on Mathematics, Computation, and Supercomputing in Nucl. Appl.*, Monterrey, CA, April 15-19, 2007, CD-ROM (2007).
4. Boukhmes Mechtoua, "Tokaimura Criticality Accident: Point Model Stochastic Neutronic Interpretation," *Trans. Am. Nucl. Society*, **84**, pp. 289-292 (2001).
5. B. G. Carlson, "Numerical Formulation and Solution of Neutron Transport Problems," Los Alamos National Laboratory report LA-2996 (1964).
6. Philippe Humbert, "Stochastic Neutronics with PANDA Deterministic Code," *Nucl. Math. And Comp. Sciences: A Century in Review, A Century Anew*, Gatlinburg, TN, April 6-11, 2003, CD-ROM (2003).
7. George I. Bell and Clarence E. Lee, "On the Probability of Initiating a Persistent Fission Chain," Los Alamos National Laboratory report LA-2608-DEL (1976).
8. M. J. D. Powell, "A Hybrid Method for Nonlinear Equations," *Numerical Methods for Nonlinear Algebraic Equations*, P. Rabinowitz, Ed., Gordon and Breach, New York, NY (1970).
9. R. J. Procassini and M. S. McKinley (editors), "The Mercury Monte Carlo Code Web Site", Lawrence Livermore National Laboratory, Web Document UCRL-WEB-212708, <http://www.llnl.gov/Mercury> (2005).
10. Raymond E. Alcouffe, Randal S. Baker, Jon A. Dahl, Scott A. Turner, and Robert C. Ward, "PARTISN: A Time-Dependent, Parallel, Neutral particle Code System," Los Alamos National Laboratory code LA-CC-08-058 (2008).

11. Mark G. Gray, "Proposed Fission Neutron Multiplicity Data in NDI," Los Alamos National Laboratory internal memorandum CCN-12:03-22, September 12, 2003 (2003).